

Convergent Expansions for Properties of the Heisenberg Model for CaV_4O_9

M. P. Gelfand,¹ Zheng Weihong,² Rajiv R. P. Singh,³ J. Oitmaa,² and C. J. Hamer²

¹*Department of Physics, Colorado State University, Fort Collins, Colorado 80523*

²*School of Physics, The University of New South Wales, Sydney, NSW 2052, Australia*

³*Department of Physics, University of California, Davis, California 95616*

(Received 1 March 1996; revised manuscript received 10 June 1996)

We have constructed high-order $T = 0$ expansions for the elementary excitation spectra, and high-temperature expansions for the susceptibility, for the $S = 1/2$ Heisenberg antiferromagnet believed to describe the spin-gap system CaV_4O_9 . Existing susceptibility data are analyzed using these theoretical results. If nearest- and second-neighbor interactions are in the ratio 2:1, there should be clear indications in both neutron and Raman scattering. [S0031-9007(96)01081-2]

PACS numbers: 75.10.Jm, 75.40.Gb

Since the discovery of high-temperature superconductivity in the cuprates, there has been much interest in two-dimensional antiferromagnetism. From a theoretical point of view, there has been an extensive search for the so-called spin liquid ground state in models with realistic interactions. A possible link between such a ground state and high-temperature superconductivity has often been suggested though not demonstrated. For square lattice Heisenberg models it is believed that sufficient further-neighbor interactions will destabilize the Néel state and lead to a spin-gap phase; however, such a phase typically has spin-Peierls order and is not a true spin liquid [1].

In light of these developments, it is interesting that the quasi-two-dimensional Heisenberg system CaV_4O_9 has been found to exhibit a spin gap [2]. Within each layer, the spins form a one-fifth depleted square lattice, which we denote the CAVO lattice (see Fig. 1). Recently, this system has attracted much attention from theorists [3–8]. It is now generally held that the spin degrees of freedom in CaV_4O_9 are in the “plaquette phase,” that is, there would be no phase transition if the intact squares (plaquettes) of the CAVO lattice were adiabatically decoupled. It has been argued [3] that the superexchange between these spins is mediated by oxygen atoms, which are situated out of the plane at the center of the squares in the CAVO lattice, and that second-neighbor interactions may be significant. It has also been suggested that the CAVO lattice is susceptible to symmetry-preserving lattice distortions [8]. Hence it is appropriate to study a Heisenberg model with interactions

$$\mathcal{H} = J_1 \sum_{(i,j)} \mathbf{S}_i \cdot \mathbf{S}_j + J'_1 \sum_{(i,k)} \mathbf{S}_i \cdot \mathbf{S}_k + J_2 \sum_{(i,l)} \mathbf{S}_i \cdot \mathbf{S}_l + J'_2 \sum_{(i,m)} \mathbf{S}_i \cdot \mathbf{S}_m, \quad (1)$$

where the sums run over nearest-neighbor bonds within plaquettes (J_1), nearest-neighbor bonds between plaquettes (J'_1), second-neighbor bonds within plaquettes (J_2), and second-neighbor bonds between plaquettes (J'_2).

We have carried out a variety of high-order convergent perturbation expansions [9–11] for this Hamiltonian that are comparable in accuracy to the best available quantum Monte Carlo calculations (which have been limited to $J_2 = J'_2 = 0$) and provide the only reliable results for the parameter values most relevant to CaV_4O_9 . These calculations include $T = 0$ expansions (i.e., Rayleigh-Schrödinger perturbation theory) about Ising models, dimer models ($J_1 = J_2 = J'_2 = 0$), and plaquette models ($J'_1 = J'_2 = 0$), as well as high-temperature expansions. In this Letter we can only describe some highlights of the results, which should be of value in guiding experimental investigations on CaV_4O_9 . We compare existing data [2] for the uniform susceptibility, $\chi(T)$, and spin gap, Δ , with those calculated theoretically, and find that the exchange parameters suggested by Ueda *et al.* [3] are consistent with the experimental energy scales. However, the detailed predictions of that model for $\chi(T)$ are not

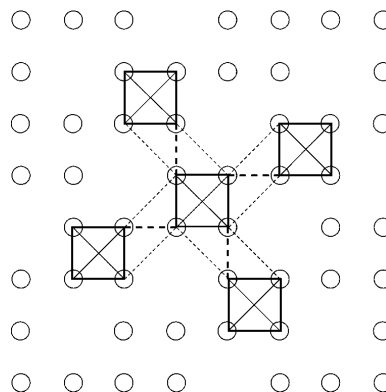


FIG. 1. The CAVO lattice, with sites indicated by circles. The couplings J_1 , J'_1 , J_2 , and J'_2 are indicated by thick solid, thick dashed, thin solid, and thin dashed lines, respectively. Note that the plaquette centers lie on a square lattice with spacing b which is $\sqrt{5}$ times the distance between nearest-neighbor sites. In characterizing the excitation spectrum we take $b = 1$ and rotate the coordinate system so that the lines between nearest-neighbor plaquette centers define the x and y axes.

entirely satisfactory, and, indeed, in the entire class of models we considered, none fits the data well over the whole temperature range 20–700 K covered by the experiment. Possible reasons for this are discussed. We then consider the excitation spectra of models described by Eq. (1). The key question at hand is whether the large spin gap is due primarily to imposed “plaquettization” (i.e., J_1 being significantly larger than J'_1) or to substantial second-neighbor interactions. We show how neutron and Raman scattering should clearly distinguish those two cases, and that particular, unusual features should be associated with the latter mechanism for the spin gap.

We begin with the high-temperature expansion for the uniform susceptibility per spin defined by the relation

$$\beta\chi(T) = \frac{1}{N} \sum_i \sum_j \langle S_i^z S_j^z \rangle, \quad (2)$$

where angular brackets represent thermal averaging and $\beta = 1/T$. The expansion coefficients have been developed for the models with $J_2 = J'_2 = 0$ and arbitrary J'_1/J_1 to order β^{14} , and with $J_1 = J'_1$ and $J_2 = J'_2 \neq 0$ to order β^{10} . Extrapolations of the former series agree well with the Monte Carlo estimates of Troyer, Kontani, and Ueda [7]. However, the resulting $\chi(T)$ does not fit the experimental data well for any choice of J'_1/J_1 . Thus we focus here on the latter series, in the hope they may be relevant to CaV_4O_9 [3].

We first compare some important energy scales from the data with the theoretical calculations to get an estimate of the exchange constants. The data are characterized by a Curie-Weiss constant $T_{\text{CW}} = 220$ K, a maximum in χ at a temperature near $T_{\text{peak}} = 110$ K and a spin gap $\Delta = 107$ K [2]. For our models, $T_{\text{CW}} = \frac{3}{4}(J_1 + J_2)$. We can estimate T_{peak} numerically by extrapolating the series expansions using differential approximants. To improve convergence, we develop approximants to $\chi e^{\Delta/T}$ rather than χ itself, with Δ taken from plaquette expansion estimates of the $T = 0$ triplet gap (described below). The resulting ratios of T_{CW} to T_{peak} are shown in Fig. 2; also shown are the values of Δ . Note that the values $J_1 \approx 200$ K and $J_2/J_1 \approx 0.5$, suggested by Ueda *et al.* [3], appear consistent with the experimental estimates of T_{CW} , T_{peak} , and Δ . However, it is not clear that the experimental estimate of T_{CW} can be taken at face value. Fitting data at finite T leads to an effective Curie-Weiss constant higher than the true one. It is plausible that the true T_{CW} for CaV_4O_9 may be (10–20)% lower than the effective value of 220 K, and this would bring the $T_{\text{CW}}/T_{\text{peak}}$ ratio closer to that expected for $J_2/J_1 \approx 0.3$.

We now consider a more detailed comparison of the theoretical $\chi(T)$ with the data. To convert the former into emu/g , we multiply our χ (calculated with $J_1 = 1$) by a factor $4N_A g^2 \mu_B^2 / J_1 k_B M$, with μ_B the Bohr magneton, k_B the Boltzmann constant, N_A Avogadro’s number, M the

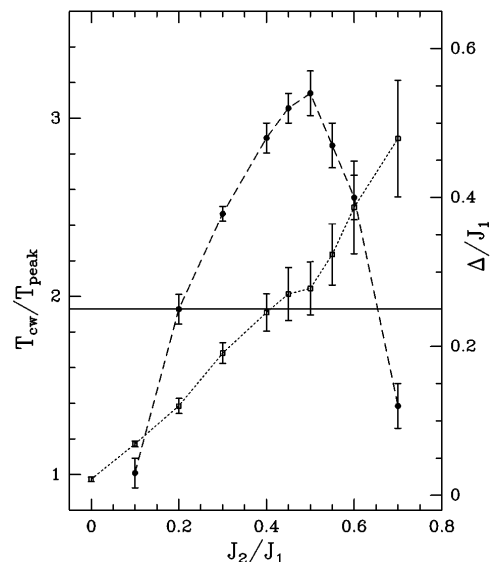


FIG. 2. Estimates of $T_{\text{CW}}/T_{\text{peak}}$ (open squares) and Δ/J_1 (filled circles) for models with $J'_1 = J_1$, $J'_2 = J_2$ plotted versus J_2/J_1 . The horizontal line indicates the value of $T_{\text{CW}}/T_{\text{peak}}$ for CaV_4O_9 (but see text for further discussion).

gram molecular weight, and the factor of 4 coming from the number of spins per CaV_4O_9 formula unit. The g factor is used as a fitting parameter; values smaller than expected (such as we find below) could, in part, reflect the presence of undetected phases which contributed to the weight but not the susceptibility.

Considering the entire temperature dependence of χ , a fair but not entirely satisfactory fit is obtained with $g = 1.78$, $J_2/J_1 = 0.5$, and $J_1 = 191$ K; we have not been able to do much better than this. Considering only the data above 200 K, reasonably good fits, optimized with respect to g and J_1 , can be found for a wide range of J_2/J_1 values. See Fig. 3 for a comparison of the data with selected fits. Even the high-temperature fits are not perfect, which is most clearly seen if one tries to fit the effective T_{CW} (which we have extracted from the data by constructing best-fit lines over restricted temperature intervals in a plot of $1/\chi$ versus T) rather than χ itself. Experimentally, the effective T_{CW} is nearly constant, at the value 220 K, for $700 > T > 475$ K. On decreasing T further the effective T_{CW} rapidly increases, reaching 330 K for $T \approx 360$ K. In contrast, the high-temperature series imply that the effective T_{CW} is analytic in $1/T$.

The difficulties we have found in fitting the $\chi(T)$ data could have several origins. We have not explored the full space of models described by Eq. (1), and there are conceivably many more symmetry-allowed terms in the spin Hamiltonian. Another possibility is that the exchange “constants” are T dependent due to spin-phonon interactions, as suggested in the present context by Starykh *et al.* [8]. We therefore turn to the calculation of excitation spectra, which can be measured by neutron

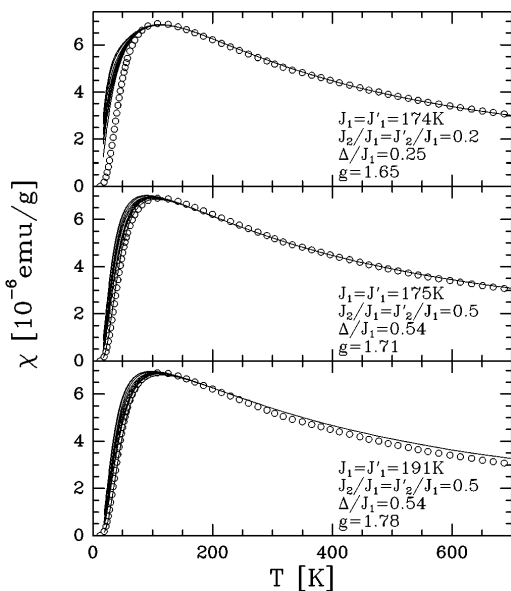


FIG. 3. Comparison of the calculated susceptibility for several Heisenberg models with parameters indicated in each panel (the solid lines representing various approximants), with the experimental data of Taniguchi *et al.* [2].

and Raman scattering and used to determine the spin Hamiltonian at low temperatures.

It is convenient to parametrize the interactions via $J_2 = \gamma J_1$, $J'_1 = \lambda_1 J_1$, and $J'_2 = \lambda_2 J_2$. We have taken $\lambda_1 = \lambda_2 \equiv \lambda$ in the calculations to be described below, but that restriction could be relaxed if desired. Note that γ specifies the intraplaquette interactions, and that we can do perturbation theory about the models with $\lambda = 0$ for any γ since they consist of disconnected plaquettes. At this point, we further restrict our attention to $\gamma < 1$, since there are ground state and lowest excited state level crossings for an isolated plaquette when $\gamma = 1$, and $\gamma < 1$ is likely more relevant to CaV_4O_9 . For an isolated plaquette, then, the ground state is a singlet, and the two lowest-lying excited states are a triplet and a singlet lying at energies J_1 and $2(1 - \gamma)J_1$ above the ground state.

For the infinite CAVO lattice, when $\lambda = 0$, the triplet elementary excitations are characterized by a flat band at energy J_1 , but as λ is increased the excitations become mobile and the band develops dispersion. Using a recently developed method for computing excitation spectra [11], the complete dispersion relation $\Delta_t(q_x, q_y)$ for triplet elementary excitations has been constructed to order λ^5 [and in some cases $O(\lambda^6)$] for various values of γ . (See the caption to Fig. 1 for the definition of the wave vectors.) Furthermore, we have been able to calculate the *singlet* excitation spectrum, $\Delta_s(q_x, q_y)$, to order λ^7 . It is not always true that these singlet excitations [which evolve from the flat band at energy $2(1 - \gamma)J_1$ when $\lambda = 0$] have the character of *elementary* excitations, since states with the same symmetry can be formed from two triplet elementary excitations. However, for γ sufficiently

large and/or λ sufficiently small, the singlet spectrum lies below the two-triplet continuum and hence represents a set of elementary excitations. More precisely, the stability criterion for the singlet elementary excitations is $2\lambda/3 < \gamma/(1 - 2\gamma)$ at small λ , and the corrections to this formula appear to be modest even for λ of order unity.

Similar plaquette expansions for the excitation spectra of the CAVO lattice Heisenberg model have been presented earlier, but only for Δ_t and only to second order in the interplaquette couplings. Katoh and Imada [4] further restricted their calculations to $\gamma = 0$, while Ueda *et al.* [3] allowed for second-neighbor interactions. The second-order results are useful as rough guides, but the high-order expansions can provide reliable, accurate results. For example, for $\gamma = 0$,

$$\begin{aligned} \Delta_t(\pi, \pi)/J_1 = & 1 - 0.666667\lambda - 0.322916\lambda^2 \\ & - 0.008186\lambda^3 + 0.033842\lambda^4 \\ & - 0.044030\lambda^5 - 0.034539\lambda^6 + \dots \end{aligned} \quad (3)$$

[Note that the second-order term in Eq. (6) of Ref. [3] is in error.] Truncating the series at $O(\lambda^2)$, one estimates that the gap vanishes at $\lambda = 1.008$. However, an exponent-biased Dlog-*Padé* analysis of all the terms leads to an estimate for the critical value of 0.920(5), which is in excellent agreement with the quantum Monte Carlo results of Troyer *et al.* [7]. Speaking more generally, it is difficult to judge the reliability of second-order perturbation theory when λ is of order unity: With higher-order terms in hand, one can be much more confident.

An interesting point which was alluded to in earlier perturbation-theoretic work [3] as well as the mean-field calculations of Starykh *et al.* [8] is that the minimum of Δ_t is not necessarily found at $\mathbf{q} = (\pi, \pi)$. For small λ , the minimum shifts from (π, π) when $\gamma < 1/2$ to $(0, 0)$ when $\gamma > 1/2$. Precisely at $\gamma = 1/2$, the minimum for small λ is achieved at (\tilde{q}, \tilde{q}) with $\tilde{q}/\pi = 0.7044\dots$. Second-order perturbation theory indicates that such incommensuration persists in a wedge in the γ - λ plane defined by $R_- \lambda \leq \frac{1}{2} - \gamma \leq R_+ \lambda$ with $R_+ \approx 0.08$ and $R_- \approx -0.32$. As λ is increased from zero the gaps tend to decrease (at least initially), and there are interesting questions about the phase diagram for γ sufficiently large that a transition to a Néel ordered state is not favored. However, we defer consideration of such matters on the grounds that they are probably not relevant to CaV_4O_9 . Instead, we will focus on the part of parameter space where the gap is large, and show that $\Delta_t(q_x, q_y)$ and $\Delta_s(q_x, q_y)$ exhibit features which are related to the strength of second-neighbor interactions.

Let us first discuss the triplet excitations. When intraplaquette and interplaquette couplings are comparable ($\lambda = 1$), the structure of $\Delta_t(q_x, q_y)$ is strongly dependent on γ : See Fig. 4 for some illustrative plots. Since one anticipates substantial spectral weight for the excitations near (π, π) , if the magnetic properties of CaV_4O_9 are

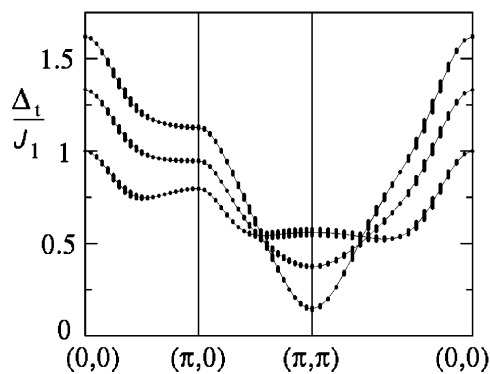


FIG. 4. The triplet excitation spectra $\Delta_t(q_x, q_y)$ along high-symmetry cuts through the Brillouin zone for coupling ratios $\lambda = 1$ and $\gamma = 0.1, 0.3,$ and 0.5 [from greatest to least values of $\Delta_t(0,0)$]. The ends of the bars indicate the values of the direct sums to fourth and fifth order in λ .

described by $\gamma \approx 0.5$ and $\lambda \approx 1$, then that nearly flat portion of its spectrum should yield a strong signature even in momentum-unresolved neutron-scattering studies. The low- T behavior of the susceptibility itself is a probe of the triplet density of states, and with sufficiently precise data it might be possible to distinguish models with a strong peak just above the gap (such as $\gamma \approx 0.5, \lambda \approx 1$) from models lacking that feature.

One spectral feature that is not evident in Fig. 4 is that when $\gamma \neq 0$ the spectra lack full square-lattice symmetry, in that $\Delta_t(q_x, q_y) \neq \Delta_t(q_y, q_x)$. This asymmetry arises at third order in λ and could not be seen in previous perturbative calculations. At $\gamma = 0.5$ and $\lambda = 1$, we estimate the asymmetry parameter

$$2 \frac{\Delta_t(q, \pi - q) - \Delta_t(\pi - q, q)}{\Delta_t(q, \pi - q) + \Delta_t(\pi - q, q)} \quad (4)$$

to have a broad maximum for $q/\pi \approx 0.3$, at the 10% level. This is a property that distinguishes between the effects of second-neighbor interactions and nonuniform nearest-neighbor couplings. Consider $\gamma \approx 0.5$ (but $\lambda \approx 1$) and $\lambda \approx 0.5$ (but γ small): In both cases the excitation bandwidth is about half J_1 , but only for the former is the asymmetry significant.

Regarding the singlet excitations, the most important point is that, if $\Delta_s(0,0)$ (which turns out to always be the minimum value of Δ_s) lies below that of any two-triplet excitations, then they should appear as sharp lines in Raman spectra [12]. At $\lambda = 1$, $\Delta_s(0,0)$ becomes less than twice the minimum Δ_t for $\gamma \approx 0.35$, and this value is, in fact, only weakly dependent on λ provided the latter is not less than 0.5. Therefore the existence of the singlet elementary excitation would be strong evidence for second-neighbor couplings playing a major role in producing the spin gap. Using the parameter estimates

of Ueda *et al.* [3] for CaV_4O_9 , the peak would lie near 100 cm^{-1} and the two-triplet continuum would have its lower edge at roughly 200 cm^{-1} .

In summary, we have carried out a wide range of high-order perturbation expansions for $S = 1/2$ Heisenberg antiferromagnets on the CAVO lattice. The existing susceptibility data for CaV_4O_9 yields energy scales which are generally consistent with the coupling ratios $J_1 = J'_1 = 2J_2 = 2J'_2$ suggested by Ueda *et al.* [3], but it seems difficult to obtain a good global fit to the $\chi(T)$ data in terms of a temperature-independent spin Hamiltonian. Neutron-scattering studies of $\Delta_t(q_x, q_y)$ can be compared with estimates of the spectrum based on the present plaquette expansions for definitive tests of models of the form (1). Raman scattering could provide evidence for an unusual magnetic elementary excitation of singlet character.

This work has been supported by the National Science Foundation under Grants No. DMR 94-57928 (M.P.G.) and No. DMR 93-18537 (R.R.P.S.). The work at UNSW is supported by a grant from the Australian Research Council. We would also like to thank M. Troyer for providing us with the Monte Carlo data, M. Sato for the experimental data on CaV_4O_9 , and D. Huse for discussions.

-
- [1] For a review, see S. Sachdev and N. Read, *Int. J. Mod. Phys. B* **5**, 219 (1991).
 - [2] S. Taniguchi *et al.*, *J. Phys. Soc. Jpn.* **64**, 2758 (1995).
 - [3] K. Ueda, H. Kontani, M. Sigrist, and P. A. Lee, *Phys. Rev. Lett.* **76**, 1932 (1996).
 - [4] N. Katoh and M. Imada, *J. Phys. Soc. Jpn.* **64**, 4105 (1995).
 - [5] K. Sano and A. Takano, Report No. cond-mat/9510160 (to be published).
 - [6] M. Albrecht and F. Mila, *Phys. Rev. B* **53**, R2945 (1996).
 - [7] M. Troyer, H. Kontani, and K. Ueda, Report No. cond-mat/9511074 (to be published).
 - [8] O. A. Starykh, M. E. Zhitomirsky, D. I. Khomskii, R. R. P. Singh, and K. Ueda, Report No. cond-mat/9601145 (to be published).
 - [9] H. X. He, C. J. Hamer, and J. Oitmaa, *J. Phys. A* **23**, 1775 (1990).
 - [10] M. P. Gelfand, R. R. P. Singh, and D. A. Huse, *J. Stat. Phys.* **59**, 1093 (1990).
 - [11] M. P. Gelfand, *Solid State Commun.* **98**, 11 (1996).
 - [12] We have not yet investigated the interactions of the triplet excitations, but we expect them to be rather weak so long as the triplet gap is large. At least we know the interactions are absent at order zero in the plaquette expansion, whereas in expansions about the Ising model, two-magnon bound states are present from the start.